Article

Stereoelectronic Effects on the Binding of Neutral Lewis Bases to CdSe Nanocrystals

Nicholas C. Anderson, Peter E. Chen, Aya K Buckley, Jonathan De Roo, and Jonathan S. Owen

J. Am. Chem. Soc., **Just Accepted Manuscript** • DOI: 10.1021/jacs.8b02927 • Publication Date (Web): 10 May 2018

Stereoelectronic Effects on the Binding of Neutral Lewis Bases to CdSe Nanocrystals

*Nicholas C. Anderson, Peter. E. Chen, Aya K. Buckley, Jonathan De Roo, Jonathan S. Owen**

Department of Chemistry, Columbia University, New York, New York, 10027.

Email: jso2115@columbia.edu, Telephone: (212) 851-5879

Abstract

Using ^{31}P nuclear magnetic resonance (NMR) spectroscopy, we monitor the competition between tri-*n*-butylphosphine (Bu_3P) and various amine and phosphine ligands for the surface of chloride terminated CdSe nanocrystals. Distinct ^{31}P NMR signals for free and bound phosphine ligands allow the surface ligand coverage to be measured in phosphine solution. Ligands with a small steric profile achieve higher surface coverages (Bu_3P = 0.5 nm^{-2}, Me_2P-*n*-octyl = 2.0 nm^{-2}, NH_2Bu = > 3 nm^{-2}) and have greater relative binding affinity for the nanocrystal (binding affinity: Me_3P > Me_2P–*n*-octyl ~ Me_2P–*n*-octadecyl > Et_3P > Bu_3P). Among phosphines, only Bu_3P and Me_2P–*n*-octyl support a colloidal dispersion, allowing a relative surface binding affinity (K_{rel}) to be estimated in that case (K_{rel} = 3.1). The affinity of the amine ligands is measured by the extent to which they displace Bu_3P from the nanocrystals (K_{rel}: H_2NBu ~ *N*-*n*-butylimidazole > 4-ethylpyridine > Bu_3P ~ $HNBu_2$ > Me_2NBu > Bu_3N). The affinity for the CdSe surface is greatest among soft, basic donors and also depends on the number of each ligand that bind. Sterically unencumbered ligands such as imidazole, pyridine, and *n*-alkylamines can therefore outcompete stronger donors such as alkylphosphines. The influence of repulsive interactions between ligands on the binding affinity is a consequence of the high atom density of binary semiconductor surfaces. The observed behavior is distinct from the self assembly of straight chain surfactants on gold and silver where the ligands are commensurate with the underlying lattice and attractive interactions between aliphatic chains strengthen the binding.

Introduction

The photoluminescence quantum yield and chemical stability of II-VI semiconductor nanocrystals depends critically on the binding affinity of their surface ligands.[1] A deeper understanding of surface coordination chemistry would aid the design of ligands that effectively stabilize nanocrystals in cellular environments and solid state lighting applications, while maximizing their photoluminescence quantum yield (PLQY). However, it is challenging to directly monitor ligand binding to surfaces in solution.

Photoluminescence spectroscopy has been used to study the binding of amines and phosphines to CdSe nanocrystals[2-10] and bulk CdSe[11-13] surfaces, where ligand binding can raise (or lower) the PLQY. For example, changes to the PLQY of a single crystal placed in an atmosphere of gaseous amine can be analyzed using the Langmuir model.[11-13] Binding constants extracted ($H_3N < H_2NMe < HNMe_2 > NMe_3$) in this manner parallel the gas phase proton affinity of the amine (with the exception of NMe_3). A similar strategy was used to analyze ligand binding to colloidal CdSe nanocrystals in solution.[14] In both cases, the PLQY is assumed to be proportional to the fractional surface coverage, which ignores several complications including changes to the recombination mechanism,[9] side reactions involving acidic impurities[15] or displacement of atoms from the crystal surface.[16] The method used to analyze single crystals also convolves the ligand donor strength and surface coverage and none measure changes to the number of accessible surface sites caused by lateral steric interactions between ligands. It is therefore unclear how to explain binding affinities that do not follow the ligand donor strength (e.g. $HNMe_2 > NMe_3$), or the relatively weak affinity of *N,N,N',N'*-tetramethylethylenediamine[16] and *bis*(diphenylphosphine)ethane[13], both of which are strong donors and have the potential ability to chelate the surface.

Nuclear magnetic resonance (NMR) spectroscopy can distinguish ligands bound to the nanocrystal surface from those freely diffusing in solution. Surface bound ligands display broad

spectral linewidths and are typically downfield of the signals from "free" ligands. Particularly for anionic ligands like alkylphosphonates and carboxylates, ligand exchange and binding can be assessed quantitatively.[17-19] However, NMR spectroscopy has been less useful for studying the exchange of neutral two electron donor ligands, e.g. *n*-alkylamines (L-type ligands)[20-22] because they undergo rapid self-exchange that causes coalescence of signals from the free and bound forms.[23-24]

We recently reported the synthesis of CdSe nanocrystals with both tri-*n*-butylphosphine (Bu_3P) and tri-*n*-butylphosphonium chloride ($[Bu_3P–H^+][Cl^-]$) ligands (**CdSe–$CdCl_2$/Bu_3P/$[Bu_3P–H]^+[Cl]^-$**). These chloride terminated nanocrystals could be prepared from carboxylate terminated CdSe nanocrystals (**CdSe–$Cd(O_2CR)_2$**) and chlorotrimethylsilane (Me_3SiCl).[25] At room temperature the exchange of the phosphine ligands is slow and distinct ^{31}P NMR signals for bound and free Bu_3P are observed. Moreover, displacement of the phosphine ligands could be monitored with ^{31}P NMR spectroscopy *in situ*. This controlled ligand exchange reactivity presents the opportunity to directly study the stereoelectronic factors that control the surface binding affinity of L-type ligands.

Results

To simplify our study, we first eliminate the oleic acid impurity that produces $[Bu_3P–H^+][Cl^-]$ by pretreatment of the nanocrystals with Me_2Cd according to a previously described method (Scheme 1).[15] After removing the solvent and any unreacted Me_2Cd, the carboxylate ligands were cleaved using Me_3SiCl and Bu_3P according to our previous study.[26] Unlike **CdSe–$CdCl_2$/Bu_3P/$[Bu_3P–H]^+[Cl]^-$**, which precipitates from pentane solution, **CdSe–$CdCl_2$/Bu_3P** is soluble in pentane and precipitates from methyl acetate or acetonitrile. A ^{31}P NMR spectrum verifies that the isolated nanocrystals are free from $[Bu_3P–H]^+[Cl]^-$ (δ = 11 ppm), and UV-Visible

absorption spectroscopy shows that the nanocrystal retain the characteristic absorption spectrum of colloidal CdSe nanocrystals without significant changes to the nanocrystal size or size distribution (Figure S1).

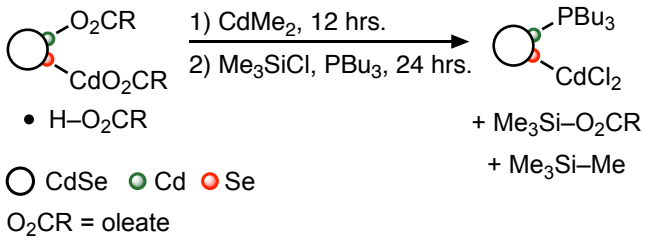

Scheme 1. Synthesis of **CdSe-CdCl$_2$/Bu$_3$P** free of [Bu$_3$PH$^+$][Cl$^-$].

To estimate the relative binding affinity of several L-type ligands, we monitored their ability to displace Bu$_3$P from **CdSe–CdCl$_2$/Bu$_3$P** (Figures S2 – S12, Table S4). For example, as *n*-octylamine is added (0 – 10 equiv./PBu$_3$), surface bound Bu$_3$P (δ = -11 ppm) is liberated producing the sharp signal of the "free" phosphine (δ = -31 ppm) (Figure 1).[27] A broadened and shifted ^{31}P NMR signal is observed when 1 – 2.5 equiv. of amine are added, suggesting that free Bu$_3$P undergoes dynamic exchange with a fraction of the surface bound ligands under these conditions. The displacement of surface bound phosphines does not influence the nanocrystal size or size distribution, as described previously. [25]

The relative surface binding affinities of the amines could be ranked by comparing the amount of Bu$_3$P displaced in the presence of tri-*n*-alkyl, di-*n*-alkyl, and *n*-alkylamines (1 or 50 equiv. / Bu$_3$P). One equiv. of *n*-butylamine more effectively displaces Bu$_3$P than does di-*n*-butylamine which is more effective than tri-*n*-butylamine. Amines with methyl substituents displace more Bu$_3$P than amines with long chain substituents (e.g. affinity of Me$_2$NBu > Bu$_3$N). These substituent effects do not follow the gas phase proton affinities nor the pK_a of the conjugate acids (pK_a(R$_3$N–H$^+$)), which are within 1 pK_a unit in water.[28] Instead they can be explained by the relative steric bulk of the incoming ligand, with the bulkiest ligands being the weakest competitors.

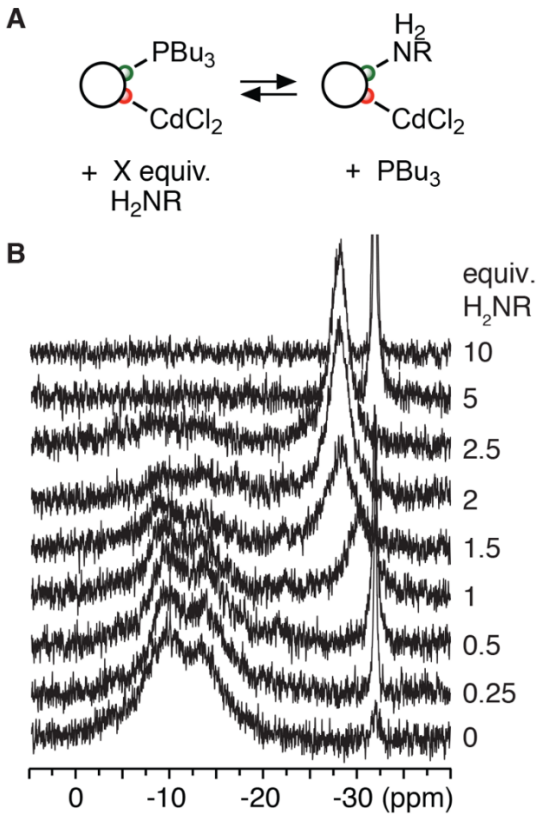

Figure 1. (A) Ligand exchange equilibrium between **CdSe-$CdCl_2$/Bu_3P** and free Bu_3P. (B) A series of ^{31}P NMR spectra of **CdSe-$CdCl_2$/Bu_3P** and increasing equivalents of added *n*-octylamine in benzene-d_6. Prior to addition of *n*-octylamine, the ^{31}P NMR spectrum shows resonances for Bu_3P bound to the CdSe nanocrystal (δ = -13 ppm) and phosphine complexes of $CdCl_2$ (δ = -9 ppm) that are associated with the nanocrystal (see ref [25]). Free Bu_3P appears at δ = -32 ppm. We assign the broadened resonance that shifts down field from free Bu_3P to a population of ligands in rapid dynamic exchange with the surface.

Similar effects were observed upon titration with tri-*n*-alkyphosphines, although in this case the surface coverage of both the incoming and outgoing ligands could be extracted from the ^{31}P NMR spectrum. In the presence of 1 equiv. of triethylphosphine (Et_3P, δ = -19 ppm), Bu_3P is displaced from the surface and the broad signal from bound phosphines shifts downfield by 5 – 10 ppm (Figure 2). Although the signals of bound Bu_3P and Et_3P overlap, their surface coverages may be determined from the amount of Bu_3P and Et_3P that remain free. Interestingly, in the presence of Et_3P (1 equiv.), the total number of bound phosphines increases from 30 ± 5 Bu_3P/nanocrystal to

36 ± 8 R_3P/nanocrystal (23 ± 5 Et_3P and 13 ± 3 Bu_3P). At higher concentrations of Et_3P more Bu_3P is displaced, however the nanocrystals begin to precipitate from the solution. Similar results are obtained with trimethylphosphine (Me_3P): in the presence of 1 equiv. of Me_3P a higher total phosphine coverage is achieved (45 ± 8 phosphines per nanocrystal). On the other hand, the coverage does not increase when Bu_3P is added, implying that the smaller phosphines can access a greater number of surface sites. We conclude that the smaller phosphines have a greater affinity for the nanocrystal.

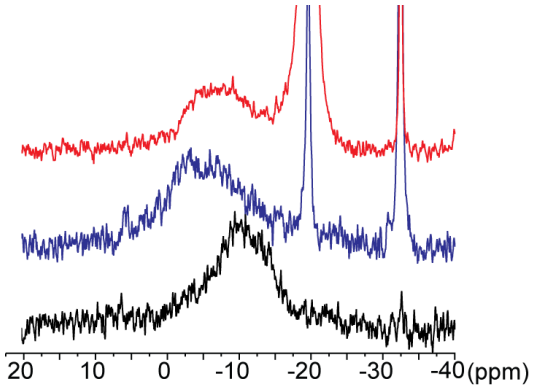

Figure 2. ^{31}P NMR spectra of **CdSe–$CdCl_2$/Bu_3P** (0.5 mM nanocrystals, 14.8 mM Bu_3P, black, bottom) with triethylphosphine (δ = -19 ppm) at 1:1 equivalents (blue) and 50:1 equivalents (red). The new broad resonance at δ = -6 ppm is Et_3P bound to the nanocrystal.

We then explored the binding of P,P-dimethyl-*n*-octylphosphine (Me_2P-*n*-octyl) with the hypothesis that this ligand would provide a stable colloidal dispersion and allow us to measure the coverage of a pure Me_2P-*n*-octyl ligand shell. Indeed, stable dispersions of Me_2P-*n*-octyl bound nanocrystals (**CdSe–$CdCl_2$/Me_2P-*n*-octyl**) could be synthesized by completely displacing Bu_3P ligands from **CdSe–$CdCl_2$/Bu_3P** or upon reaction of **CdSe–$Cd(O_2CR)_2$**, with Me_2P-*n*-octyl and Me_3SiCl (see Supporting Information, Figure S13). By either method, the Me_2P-*n*-octyl surface coverage is 2.0 – 2.2 nm^{-2} (90 ± 15 Me_2P-*n*-octyl per nanocrystal, d = 3.8 nm, see Supporting Information), ~4x greater than the coverage of Bu_3P ligands. From the saturation coverages of Bu_3P

and Me_2P-*n*-octyl, a competitive binding model could be used to measure the relative affinity (see Supporting Information).[29] The ratio of binding constants ($K_{rel} = K_1/K_2$) for the incoming (L_1) and outgoing (L_2) ligand can be calculated from the molar concentration of the free ligands ($[L_i]$) and their fractional coverage (θ_i) in a solution of both competing ligands according to Equation 1.

$$K_{rel} = \frac{K_1}{K_2} = \frac{\theta_1 [L_2]}{\theta_2 [L_1]} \qquad (1)$$

The θ_i of Me_2P-*n*-octyl and Bu_3P is calculated by dividing the coverage of each phosphine in the mixture by the saturation coverage of the pure ligand shell. From this analysis Me_2P-*n*-octyl has a surface binding affinity ~3x greater than Bu_3P. Because K_i is normalized by the number of binding sites accessible to each ligand, the difference in affinity reflects the binding characteristics on a per ligand basis. Thus, the 3x greater affinity of Me_2P-*n*-octyl may be attributed to a weaker repulsive interaction of its substituents with neighboring phosphines or the nanocrystal surface. On the other hand, Eq. 1 assumes that a single binding constant applies at all coverages. If the acidity of the nanocrystal decreases as the number of surface bound ligands grows the binding affinity will decrease. This effect can influence the magnitude of intermediate coverages obtained in equimolar solutions of Me_2P-*n*-octyl and Bu_3P will increase the affinity of Me_2P-*n*-octyl and reduce the affinity of Bu_3P relative to their affinity at saturation. More detailed investigations of the binding energy as a function of the coverage and ligand structure are required to assess these issues.

A wide range of ligands were surveyed using the approaches described above. The relative affinity of the tri-*n*-alkylphosphines is Me_3P > Me_2P-*n*-octyl > Et_3P > Bu_3P while the affinity of the amine ligands is H_2NBu > Bu_3P ~ $HNBu_2$ > Me_2NBu > NBu_3. Previous studies that used the photoluminescence intensity from single crystals[12, 30] and colloidal nanocrystals[14] to monitor ligand binding report similar trends in the affinity of mono-, di-, and trisubstituted *n*-alkylamines despite the fact that they do not deconvolute variations in the ligand coverage from the relative binding

affinities. In addition to the ligands described above, a variety of bulky and/or electron deficient ligands displace little or no Bu_3P from the nanocrystals even at high concentration, including triethylphosphite, triphenylphosphine, diphenylphosphine, tetradecanol, furan, thiophene, tetrahydrofuran, diethylether, *n*-pentylisocyanide, and di-*n*-butylsulfide.

To assess the effect of ligand basicity and structure on the displacement reactivity, the pK_a of the conjugate acid and the Tolmann cone angle of each ligand are plotted in Figure 3.[31-32] Ligands that effectively compete with Bu_3P for the nanocrystal surface are highlighted. Both a small cone angle and a high ligand basicity are key to a high affinity for the surface. Sterically unencumbered ligands with low basicity, such as *n*-pentylisocyanide (pK_a(R–N≡C–H^+) = 0.86, H_2O, R = cyclohexyl)[33] are weak competitors. However, a weak basicity is partly overcome if the donor atom is soft, as in the case of tetrahydrothiophene (pK_a(Et_2S–H^+) = -6.7, H_2O)[34], which displaces Bu_3P at high concentration. The special affinity of soft ligands helps explain the poor binding of the hard Bu_3N ligand (pK_a(Et_3N–H^+) = 10.7, H_2O)[34], which is a stronger Brønsted base than its isostructural phosphine (pK_a(Bu_3P–H^+) = 8.4, H_2O)[32]. Bu_3N also has a greater cone angle than Bu_3P, owing to the shorter M–N bond and the larger C–E–C angle, which increases its steric profile. Thus, soft, basic ligands with a small steric profile bind with the greatest affinity.

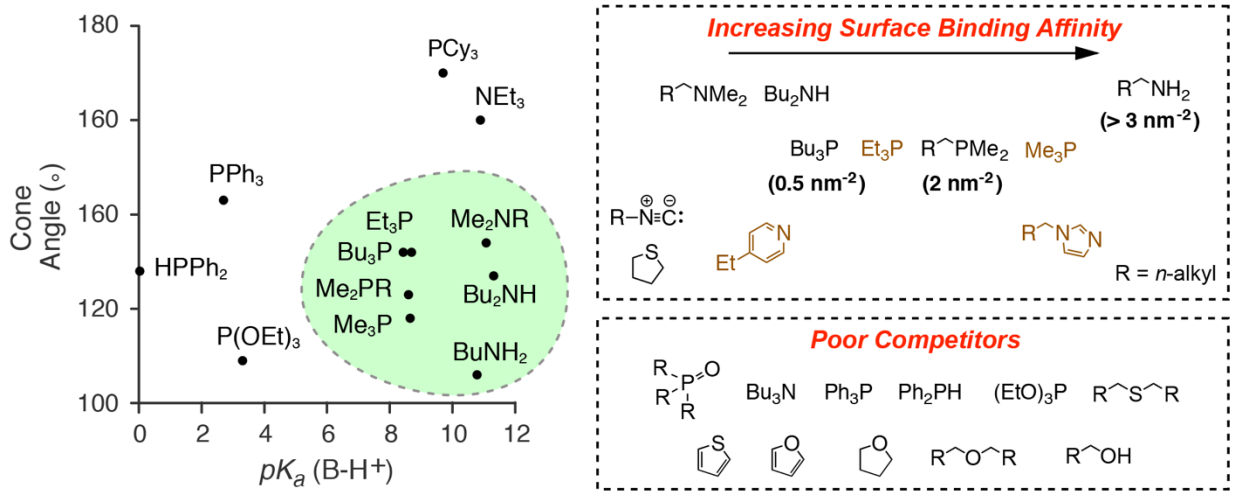

Figure 3. (left) pK_a *versus* Tolmann cone angles for amines and phosphines in the ligand binding series. The green area contains strong binders. (right, top) Relative binding affinities of all molecules studied, with molecules of greatest affinity on the right. Molecules in brown do not support stable colloidal dispersion on their own. (right, bottom) Molecules that do not displace significant quantities of Bu_3P at high concentration. In all cases, R = *n*-alkyl.

Pyridine and tri-*n*-octylphosphine oxide (TOPO) have been reported to stabilize nanoparticle dispersions, although recent studies argue otherwise.[35-38] To shed light on the issue we studied the displacement of Bu_3P from **CdSe–$CdCl_2$/Bu_3P** in pyridine and TOPO solution. Despite its moderate basicity, pyridine (pK_a(pyridine–H^+) = 5.2, H_2O)[39] effectively displaces the much more basic and soft Bu_3P donor ligand. In the presence of 1 equiv. of pyridine, the nanocrystals begin to precipitate. However, 1 equiv. of 4-ethylpyridine displaces 30% of the Bu_3P and maintains a stable dispersion. Higher concentrations of 4-ethylpyridine also induce precipitation. Similar results are observed with 1-*n*-butylimidazole, which outcompetes Bu_3P for the nanocrystal surface and displaces a greater quantity of Bu_3P than does pyridine, consistent with its greater basicity (pK_a(imidazole–H^+) = 7.0, H_2O) and small steric profile. TOPO, on the other hand, does not displace Bu_3P, even at high concentrations (0.3 M). Moreover, the reaction of **CdSe-$Cd(O_2CR)_2$** with Me_3SiCl in pyridine or TOPO solution caused precipitation of the nanocrystals. We conclude that pyridine and 1-butylimidazole bind the nanocrystal surface effectively but do not stabilize a colloidal dispersion, even in a neat solution of the ligand. On the other hand, TOPO does not compete with Bu_3P, nor does it stabilize a colloidal dispersion.

The relatively high affinity of the pyridine and imidazole ligands, and the influence of steric properties on the coverage of alkylphosphines and amines suggests that the competitive binding equilibrium is determined by the number of each competitor that binds as well as the relative surface–ligand bond dissociation energy (BDE(S–L)). The surface coverages vary widely depending on the steric properties of the ligand. The coverage of phosphines increases 4-fold on

exchanging Bu_3P for Me_2P-*n*-octyl (0.5 nm^{-2} vs. 2 nm^{-2}). These coverages are somewhat insensitive to the solution concentration and appear near the maximum coverages for these ligands. *n*-Alkylamines, on the other hand, display concentration dependent binding - poor colloidal stability is observed as the amine concentration is lowered - and their rapid degenerate exchange prevents the coverage from being directly measured *in situ* using ^{1}H NMR spectroscopy. A lower bound for their saturation coverage can be estimated by precipitating the nanocrysatls from concentrated amine solution, drying them under vacuum, and measuring the amine content of the isolated product (see Supporting Information). A range of coverages determined this way suggest the saturation coverage of *n*-alkylamines is greater than > 3 nm^{-2}. This is similar to typical coverages of *n*-alkylcarboxylates following careful purification (3 – 3.5 carboxylates/nm^{-2}).[15-16, 25] Thus, ligands with a smaller effective cross-sectional area can form a greater number of surface ligand bonds and, in principle, compensate for a weak surface–ligand interaction. This helps explain the affinity of relatively weak donors such as pyridine and *n*-pentylisocyanide. On the contrary, strong donors, such as trialkylamines and *N*-heterocylic carbenes (NHCs) (pK_a(NHC–H^+) ~ 23)[40] may form a strong surface–ligand bond, but achieve low coverages when their substituents are bulky (e.g. mesityl). Nonetheless, NHCs form especially stable monolayers on gold surfaces that are resistant to displacement by sterically unencumbered thiols.[41] In all cases, to understand the binding affinity one must assess both the saturation coverage as well as the BDE(S–L).

The precipitation caused by displacing Bu_3P with pyridine confirms a recent study of stoichiometric CdSe nanocrystals bound only by *n*-alkylamine ligands.[15] That study suggested that previously reported dispersions stabilized by pyridine are aided by acidic impurities that contribute electrostatic stabilization.[10, 42-48] The same study also reported that stoichiometric CdSe nanocrystals stabilized by Bu_3P alone (**CdSe–Bu_3P**) were unstable to aggregation, which is at odds with the stability of **CdSe–$CdCl_2$/Bu_3P** herein.[15, 25] Interestingly, adding $CdCl_2$ to partially

aggregated **CdSe–Bu$_3$P**[15] forms a clear, stable dispersion that is indistinguishable from the **CdSe–CdCl$_2$/Bu$_3$P** used in this study (See Supporting Information). The mechanism by which $CdCl_2$ improves the colloidal stability is unclear and the subject of current investigations in our lab.

Given the high binding affinities and increased surface coverages of sterically unencumbered ligands observed above, we sought to stabilize stoichiometric CdSe nanocrystals in the absence of $CdCl_2$ using *P,P*-dimethyl-*n*-octadecylphosphine (Me_2P-*n*-octadecyl). **CdSe–Me$_2$P-*n*-octadecyl** was prepared from **CdSe–NH$_2$Bu**[15] *via* ligand exchange. Addition of Me_2P-*n*-octadecyl to **CdSe–NH$_2$Bu** in C_6D_6 does not displace *n*-butylamine, as expected from the relative binding affinities measured above (Figure 3), until the primary amine is removed under vacuum with heat (See Supporting Information). Binding of the Me_2P-*n*-octadecyl ligand can be monitored by the appearance of a broad ^{31}P NMR resonance (δ = -38 ppm, $\Delta\delta$ = 15 – 20 ppm) that increases in intensity as the amine ligands are desorbed. Following complete removal of NH_2Bu, stable colloidal dispersions are obtained. The Me_2P-*n*-octadecyl coverage reaches 2 nm^{-2}, similar to the coverage of phosphine ligands in **CdSe–CdCl$_2$/Me$_2$P-*n*-octyl**. We conclude that the higher ligand coverage and the long *n*-octadecyl chain provide greater colloidal stability to **CdSe–Me$_2$P-*n*-octadecyl** compared to **CdSe–Bu$_3$P**.

Interestingly, Me_2P–*n*-octadecyl undergoes slow degenerate ligand exchange with **CdSe–Me$_2$P-*n*-octadecyl** on the NMR timescale. Even at temperatures as high as 390 K, the average Me_2P–*n*-octadecyl exchange rate constant is lower than 10^{-3} s^{-1} (see Supporting Information). This suggests that phosphines form stronger surface ligand bonds than *n*-alkylamines, which undergo fast degenerate exchange on the ^1H NMR timescale at room temperature.[23-24] Similarly, phosphines are known to bind aqueous Cd^{2+} more tightly than isostructural amines.[49-50] Thus, we tentatively conclude that tri-*n*-alkylphosphine ligands have a greater BDE(S–L) than primary *n*-alkylamine ligands, yet their affinity for the surface is lower because primary *n*-alkylamines achieve higher

surface coverages, as depicted in the table of contents graphic. To properly assess their relative BDE(S–L), it will be important to measure the relative binding of these ligands at the same surface coverage, and ideally at multiple coverages for the reasons related to the surface coverage dependent affinity discussed above.

In all cases described herein, the surface ligand coverages are significantly lower than the aerial density of atoms on the CdSe surface (5.4 – 6.2 nm^{-2}) and the packing density of crystalline alkane chains (4.9 nm^{-2}). These low coverages suggest that repulsive interactions between ligands can block adjacent binding sites and many binding sites will remain uncoordinated. While surface coverages higher than the areal density of crystalline alkanes or binding sites on the crystal surface are sometimes reported, these values may reflect the formation of multilayers or the presence of free ligands, rather than the number of surface–ligand bonds.[51] On the other hand, the highly curved surfaces of very small nanocrystals can accommodate a greater number of surface ligands. For example, pyramidal CdSe clusters with 1.7 – 2.5 nm edge lengths have 1.5 – 2x increased volume available for their ligands compared to a flat facet and one benzoate or *n*-butylamine ligand can bind every available coordination site.[52] These high ligand coverages are thought to stabilize their so called "magic" sizes. However, as the particle size increases and the curvature drops, the packing of ligands must fall below that of crystalline *n*-alkanes (4.9 nm^{-2}). Thus, the high atom density of surfaces causes steric interactions between ligands that reduces their packing on the nanocrystal surface and lowers their surface binding affinity.

Self-assembled monolayers (SAMs) pack with aerial densities (4 – 4.6 nm^{-2}) just below those of crystalline alkanes.[53-56] On the Au(111) surface, thiolate SAMs assume high symmetry, crystalline structures that are commensurate with the underlying lattice, but much less densely packed (4.6 nm^{-2}) than the surface atoms (12 atoms nm^{-2}). Van der Waals interactions between chains within the SAM strengthen the binding and increase as the chain length grows.[57-58] However,

the Si(111) surface has an aerial density of atop sites (7.8 nm^{-2}) that is greater than the maximum packing density of alkane chains. Each surface atom on Si(111) presents a single dangling bond that can be terminated by a Si–H or Si–Me bond, however larger functional groups, such as ethyl, do not form a complete monolayer.[59] Moreover, theoretical and experimental work has shown that the rotation of methyl groups on Si(111) is hindered by steric interactions with neighboring methyls.[60] In both cases interactions between neighboring ligands dictate the coverage and structure of these surface layers.

On the surfaces of II-VI and III-V nanocrystals, the areal densities of surface atoms are equal to or lower than Si(111), but still greater than the crystalline alkanes in most cases. Even straight chain ligands such as NH_2Bu will not bind every available site as the surfaces grow beyond a few nanometers. In addition, amine and phosphine ligands typically form a single dative bond while the [100] surface presents two dangling bonds per surface atom. Thus, the surfaces of colloidal nanocrystals will contain many vacant coordination sites if organic ligands are the exclusive surface binding agent. Nanocrystals stabilized solely by sterically bulky ligands (e.g. Bu_3P), can, therefore, be expected to contain even greater numbers of vacant coordination sties. As a result, there is a significant driving force to displace large bulky ligands and increase the number of surface ligand bonds. Thus, the steric size of the ligand strongly influences its ligand binding affinity.

Conclusion

The stereoelectronic properties of amines and phosphines were surveyed using competitive binding experiments. Soft, electron rich donor ligands bind the surface most tightly making phosphines a better ligand than their isostructural amines. However, the surface coverage of ligands is very sensitive to their steric bulk with coverages varying by 6x or more depending on the ligand

structure. The large difference in the number of surface–ligand bonds has a significant impact on the competitive binding equilibrium, such that analyzing donor strength of the ligand alone is not sufficient to determine which ligands have a high binding affinity. Hence a strong Lewis base may therefore be readily displaced from the surface by weaker Lewis base with a smaller steric profile. The displacement of Bu_3P by pyridine, a much harder and weaker Lewis base, is a good example of this reactivity. The impact of steric bulk on the coverage and competitive binding is expected for all the binary semiconductor crystals whose surface atoms are more densely packed than crystalline alkane chains, particularly as the nanocrystal grows larger than a few nm.

Acknowledgements

This work was supported by the Department of Energy (Grant No. DE-SC0006410). Nicholas Anderson and Peter Chen were supported by National Science Foundation Graduate Research Fellowships (Grant No. DGE07-07425 and DEG11-44155, respectively). Jonathan De Roo acknowledges support from the Belgian American Education Foundation (BAEF), Fulbright and the European Union's Framework Program for Research and Innovation Horizon 2020 (2014-2020) under the Marie Skłodowska-Curie Grant Agreement COMPASS No. 691185. The authors acknowledge Ponisseril Somasundaran for helpful discussions.

Methods

General Considerations. All manipulations were performed using standard Schlenk techniques or within a nitrogen atmosphere glovebox unless otherwise indicated. Pentane, toluene, methyl acetate, diethyl ether and tetrahydrofuran were purchased anhydrous from Sigma Aldrich and shaken over activated alumina, filtered, and stored over 4 Å molecular sieves in an inert atmosphere glovebox at least 24 h prior to use. Diphenylphosphine (99%), *N,N,'N,'N*-tetramethylethylene-1,2-diamine (TMEDA) (98%), triethylphosphite (99%), tri-*n*-octylphosphine (97%), triethylphosphine (99%), and tri-*n*-butylphosphine (99%) were purchased from Strem and used without further purification. $CdMe_2$ was purchased from Strem and vacuum distilled prior to use. *CAUTION: Dimethylcadmium is extremely toxic and because of its volatility and air-sensitivity should only be handled by a highly trained and skilled scientist. N,N*-Dimethylbutylamine (98%), furan (99%), thiophene (98%), *n*-butylamine (98%), di-*n*-butylamine (98%), trimethylphosphine (99%), , *n*-pentylisocyanide, di-*n*-butylsulifide (98%), trichloromethylsilane (98%), tri-*n*-butylamine (99%), *n*-octylamine (99%), benzene-d_6 (99.9%) and pyridine (99.5%) were purchased from Sigma Aldrich and dried over CaH_2, distilled, and stored in a nitrogen glovebox. Toluene-d_8 was purchased from Cambridge Isotopes and dried over CaH_2, distilled, and stored in a nitrogen glovebox. Tri-*n*-octylphosphine oxide (99%) was purchased from Sigma Aldrich and recrystallized from acetonitrile as reported previously.(34)

CdSe–Cd(O$_2$CR)$_2$. Carboxylate terminated CdSe nanocrystals (**CdSe–Cd(O$_2$CR)$_2$**) are synthesized and treated with Me_2Cd to remove acidic impurities as previously described.[61]

CdSe–CdCl$_2$/Bu$_3$P. All manipulations are conducted on a Schlenk line at room temperature. In a typical synthesis, a benzene-d_6 stock solution of **CdSe–Cd(O$_2$CR)$_2$** (1.0 ml, 0.5 – 2.0 mmolar carboxylate, [CdSe] = 1.6 – 6.5 mmolar, [nanocrystal] = 4 – 16 μmolar) was transferred to a 50 ml Schlenk tube with a magnetic stir bar. The solution was diluted to a total volume of 5 ml with toluene to which Bu_3P (0.506 g, 0.624 ml, 2.5 mmol) was added. Me_3Si–Cl (6.0 – 24 mmol, 12 equiv.) was added and the solution stirred for 24 hours. After this time, the volatiles were removed under vacuum and the red solid dissolved in pentane (5 ml) and a methyl acetate was added to precipitate the nanocrystals, which were separated by centrifugation (7000 RPM for 5 minutes). This process was repeated twice more, after which the red powder was dried overnight under vacuum. The nanocrystals were dispersed in benzene-d_6 to a CdSe concentration of 0.5 – 1.0 M, as described previously.[16]

Competitive Displacement of Bu$_3$P from CdSe–CdCl$_2$/Bu$_3$P. Benzene-d_6 stock solutions of various competitor ligands are prepared in a nitrogen filled glove box by diluting the ligand (0.9 mmole) with benzene-d_6 (1 ml). Using a 25 μl syringe, 10 μl of this stock solution (9 μmoles of ligand) is added to a benzene-d_6 solution of **CdSe-CdCl$_2$/Bu$_3$P** (600 μl, 15 mM in Bu_3P, 0.6 mM in nanocrystal) in a J-young NMR tube to form an equimolar solution of the added ligand and Bu_3P. $^{31}P\{^1H\}$ and ^1H NMR spectra are acquired within 1 hour ($^{31}P\{^1H\}$: 2 sec delay with 0.1 sec acquisition, 800 scans; ^1H: 30 sec delay with 5 sec acquisition, 16 scans). The J-young tube is then transferred to a nitrogen filled glove box where the appropriate mass of neat ligand is added to bring the total concentration of ligand to 0.75 M (50 equiv.). The J-young tube is then sealed and $^{31}P\{^1H\}$ and ^1H NMR spectra are acquired as described above. In some cases the procedure is reapeated to bring the concentration of competitor ligand to 1.5 M (100 equiv.).

***P,P*-Dimethyl-*n*-octylphosphine.** *P,P*-dimethyl-*n*-octylphosphine was prepared on 19.7 mmole scale from *n*-octylmagnesium bromide and chlorodimethylphosphine as previously described.[62] $^{31}P\{^{1}H\}$ NMR (C_6D_6, 162 MHz): δ = -55 ppm, (chloroform-*d*, 162 MHz): δ = -51 ppm. ^{1}H NMR (chloroform-*d*, 400 MHz): δ = 0.89 (d, 6H, -CH_3), 0.91 (t, 3H, -CH_3) 1.2-1.6 (b, 12H, -CH_2), 1.59 (m, 2H, β-CH_2), 1.98 (m, 2H, -PCH_2). $^{31}P\{^{1}H\}$ NMR (s).

Synthesis of CdSe–$CdCl_2$/Me_2P–*n*-octyl. All manipulations were conducted on a Schlenk line at room temperature. In a typical synthesis, a benzene-d_6 stock solution of **CdSe–Cd(O_2CR)$_2$** (1.0 ml, 0.5–2.0 mmol ligand) with a known carboxylate concentration was transferred to a 50 ml Schlenk tube with a magnetic stir bar. The solution was diluted to a total volume of 5 ml with toluene to which Me_2P-*n*-octyl (0.438 g, 2.5 mmol) was added. Me_3Si–Cl (0.651 – 2.607 g, 6.0 – 24 mmol, 12 equiv.) was added and the solution stirred for 24 hours. After this time, the volatiles were distilled off under vacuum and the red solid dissolved in toluene (5 ml) and methyl acetate was added to precipitate the nanocrystals, which were separated by centrifugation (7000 RPM for 5 minutes). This process was repeated twice more, after which the red powder was dried overnight under vacuum. The nanocrystals were diluted in toluene-d_8 to [nanocrystal] = 0.5 – 1.0 mM and analyzed $^{31}P\{^{1}H\}$ and ^{1}H NMR spectroscopies.

Supporting Information

Variable temperature NMR spectroscopy of **CdSe–$CdCl_2$/Me_2P–*n*-octyl**, the synthesis of **CdSe–$CdCl_2$/PBu_3** from **CdSe–NH_2Bu**, the synthesis of Me_2P–*n*-octadecylphosphine and the synthesis of **CdSe–Me_2P–*n*-octadecylphosphine** are described in the supporting information.

References

1. Owen, J., The coordination chemistry of nanocrystal surfaces. *Science* **2015,** *347* (6222), 615-616.
2. Munro, A. M.; Plante, I. J.-l.; Ng, M. S.; Ginger, D. S., Quantitative Study of the Effects of Surface Ligand Concentration on CdSe Nanocrystal Photoluminescence. *Journal of Physical Chemistry C* **2007,** *33*, 6220-6227.
3. Kalyuzhny, G.; Murray, R. W., Ligand effects on optical properties of CdSe nanocrystals. *The journal of physical chemistry. B* **2005,** *109*, 7012-7021.
4. Jasieniak, J.; Mulvaney, P., From Cd-rich to Se-rich - The manipulation of CdSe nanocrystal surface stoichiometry. *Journal of the American Chemical Society* **2007,** *129* (10), 2841-2848.
5. Galian, R. E.; Scaiano, J. C., Fluorescence quenching of CdSe quantum dots by tertiary amines and their surface binding effect. *Photochem. Photobiol. Sci.* **2009,** *8* (1), 70-74.
6. Gomez, D. E.; van Embden, J.; Jasieniak, J.; Smith, T. A.; Mulvaney, P., Blinking and surface chemistry of single CdSe nanocrystals. *Small* **2006,** *2* (2), 204-208.
7. Bawendi, M. G.; Carroll, P. J.; Wilson, W. L.; Brus, L. E., LUMINESCENCE PROPERTIES OF CDSE QUANTUM CRYSTALLITES - RESONANCE BETWEEN INTERIOR AND SURFACE LOCALIZED STATES. *J. Chem. Phys.* **1992,** *96* (2), 946-954.
8. Murray, C. B.; Norris, D. J.; Bawendi, M. G., Nanocrystallites, Te Semiconductor. *Journal of the American Chemical Society* **1993,** *115*, 8706-8715.
9. Busby, E.; Anderson, N. C.; Owen, J. S.; Sfeir, M. Y., Effect of Surface Stoichiometry on Blinking and Hole Trapping Dynamics in CdSe Nanocrystals. *Journal of Physical Chemistry C* **2015,** *119* (49), 27797-27803.
10. Guyot-Sionnest, P.; Shim, M.; Matranga, C.; Hines, M., Intraband relaxation in CdSe quantum dots. *Phys. Rev. B* **1999,** *60* (4), R2181-R2184.

11. Meeker, K.; Ellis, A. B., Adsorption of Alkanolamines onto Semiconductor Surfaces: Cadmium Selenide Photoluminescence as a Probe of Binding and Film Reactivity toward Carbon Dioxide. *The Journal of Physical Chemistry B* **1999,** *103* (6), 995-1001.
12. Meyer, G. J.; Lisensky, G. C.; Ellis, A. B., Evidence for Adduct Formation at the Semiconductor Gas Interface - Photoluminescent Properties of Cadmium Selenide in the Presence of Amines. *Journal of the American Chemical Society* **1988,** *110* (15), 4914-4918.
13. Murphy, C. J.; Ellis, A. B., The coordination of mono- and diphosphines to the surface of cadmium selenide. *Polyhedron* **1990,** *9* (15), 1913-1918.
14. Bullen, C.; Mulvaney, P., The effects of chemisorption on the luminescence of CdSe quantum dots. *Langmuir* **2006,** *22* (7), 3007-3013.
15. Chen, P. E.; Anderson, N. C.; Norman, Z. M.; Owen, J. S., Tight Binding of Carboxylate, Phosphonate, and Carbamate Anions to Stoichiometric CdSe Nanocrystals. *Journal of the American Chemical Society* **2017,** *139* (8), 3227-3236.
16. Anderson, N. C.; Hendricks, M. P.; Choi, J. J.; Owen, J. S., Ligand Exchange and the Stoichiometry of Metal Chalcogenide Nanocrystals: Spectroscopic Observation of Facile Metal-Carboxylate Displacement and Binding. *Journal of the American Chemical Society* **2013,** *135* (49), 18536-18548.
17. Fritzinger, B.; Capek, R. K.; Lambert, K.; Martins, J. C.; Hens, Z., Utilizing Self-Exchange To Address the Binding of Carboxylic Acid Ligands to CdSe Quantum Dots. *Journal of the American Chemical Society* **2010,** *132* (29), 10195-10201.
18. De Roo, J.; Van Driessche, I.; Martins, J. C.; Hens, Z., Colloidal metal oxide nanocrystal catalysis by sustained chemically driven ligand displacement. *Nat Mater* **2016,** *15* (5), 517-521.
19. Valdez, C. N.; Schimpf, A. M.; Gamelin, D. R.; Mayer, J. M., Low Capping Group Surface Density on Zinc Oxide Nanocrystals. *ACS Nano* **2014,** *8* (9), 9463-9470.
20. Green, M. L. H.; Parkin, G., Application of the Covalent Bond Classification Method for the Teaching of Inorganic Chemistry. *J. Chem. Educ.* **2014,** *91* (6), 807-816.
21. Green, M. L. H., A NEW APPROACH TO THE FORMAL CLASSIFICATION OF COVALENT COMPOUNDS OF THE ELEMENTS. *J. Organomet. Chem.* **1995,** *500* (1-2), 127-148.
22. De Roo, J.; De Keukeleere, K.; Hens, Z.; Van Driessche, I., From ligands to binding motifs and beyond; the enhanced versatility of nanocrystal surfaces. *Dalton Trans* **2016,** *45* (34), 13277-83.
23. Ji, X. H.; Copenhaver, D.; Sichmeller, C.; Peng, X. G., Ligand bonding and dynamics on colloidal nanocrystals at room temperature: The case of alkylamines on CdSe nanocrystals. *Journal of the American Chemical Society* **2008,** *130* (17), 5726-5735.
24. Fritzinger, B.; Moreels, I.; Lommens, P.; Koole, R.; Hens, Z.; Martins, J. C., In Situ Observation of Rapid Ligand Exchange in Colloidal Nanocrystal Suspensions Using Transfer NOE Nuclear Magnetic Resonance Spectroscopy. *Journal of the American Chemical Society* **2009,** *131* (8), 3024-3032.
25. Anderson, N. C.; Owen, J. S., Soluble, Chloride-Terminated CdSe Nanocrystals: Ligand Exchange Monitored by H-1 and P-31 NMR Spectroscopy. *Chem. Mat.* **2013,** *25* (1), 69-76.
26. Goyal, A.; Kang, S.; Leonard, K. J.; Martin, P. M.; Gapud, A. A.; Varela, M.; Paranthaman, M.; Ijaduola, A. O.; Specht, E. D.; Thompson, J. R.; Christen, D. K.; Pennycook, S. J.; List, F. A., Irradiation-free, columnar defects comprised of self-assembled nanodots and nanorods resulting in strongly enhanced flux-pinning in YBa2Cu3O7-delta films. *Supercond. Sci. Technol.* **2005,** *18* (11), 1533-1538.
27. At equimolar amine, a broadened signal appears at a chemical shift between free and surface bound phosphine that we tentatively assign to Bu3P ligands in rapid exchange with a fraction of the surface bound phosphines. However, this interpretation is complicated by Bu3P complexes of CdCl2 that are also present in the reaction mixture (see ref. X). .
28. Trotman-Dickenson, A. F., The Basic Strength of Amines. *J Chem Soc* **1949,** (May), 1293-1297.
29. Kroupa, D. M.; Anderson, N. C.; Castaneda, C. V.; Nozik, A. J.; Beard, M. C., In situ spectroscopic characterization of a solution-phase X-type ligand exchange at colloidal lead sulphide quantum dot surfaces. *Chemical Communications* **2016,** *52* (96), 13893-13896.
30. Lisensky, G. C.; Penn, R. L.; Murphy, C. J.; Ellis, A. B., Electrooptical Evidence for the Chelate Effect at Semiconductor Surfaces. *Science* **1990,** *248* (4957), 840-843.

31. Brown, T. L.; Lee, K. J., Ligand steric properties. *Coordination Chemistry Reviews* **1993,** *128* (1), 89-116.
32. Rahman, M. M.; Liu, H. Y.; Eriks, K.; Prock, A.; Giering, W. P., Quantitative analysis of ligand effects. Part 3. Separation of phosphorus(III) ligands into pure .sigma.-donors and .sigma.-donor/.pi.-acceptors. Comparison of basicity and .sigma.-donicity. *Organometallics* **1989,** *8* (1), 1-7.
33. Sung, K. S.; Chen, C. C., Kinetics and mechanism of acid-catalyzed hydrolysis of cyclohexyl isocyanide and pK(a) determination of N-cyclohexylnitrilium ion. *Tetrahedron Lett* **2001,** *42* (29), 4845-4848.
34. Laurence, C.; Gal, J.-F. o., *Lewis basicity and affinity scales : data and measurement*. John Wiley: Chichester, West Sussex, U.K., 2010; p xv, 460 p., 12 p. of plates.
35. Owen, J. S.; Park, J.; Trudeau, P.-E.; Alivisatos, a. P., Reaction chemistry and ligand exchange at cadmium-selenide nanocrystal surfaces. *Journal of the American Chemical Society* **2008,** *130*, 12279-12281.
36. Kopping, J. T.; Patten, T. E., Identification of acidic phosphorus-containing ligands involved in the surface chemistry of CdSe nanoparticles prepared in tri-N-octylphosphine oxide solvents. *Journal of the American Chemical Society* **2008,** *130*, 5689-5698.
37. Wang, F.; Tang, R.; Buhro, W. E., The Trouble with TOPO; Identification of Adventitious Impurities Beneficial to the Growth of Cadmium Selenide Quantum Dots, Rods, and Wires. *Nano Letters* **2008,** *8* (10), 3521-3524.
38. Wang, F.; Tang, R.; Kao, J. L.-F.; Dingman, S. D.; Buhro, W. E., Spectroscopic identification of tri-n-octylphosphine oxide (TOPO) impurities and elucidation of their roles in cadmium selenide quantum-wire growth. *Journal of the American Chemical Society* **2009,** *131*, 4983-4994.
39. Bordwell, F. G., Equilibrium Acidities in Dimethyl-Sulfoxide Solution. *Accounts Chem Res* **1988,** *21* (12), 456-463.
40. Amyes, T. L.; Diver, S. T.; Richard, J. P.; Rivas, F. M.; Toth, K., Formation and stability of N-heterocyclic carbenes in water: The carbon acid pK(a) of imidazollum cations in aqueous solution. *Journal of the American Chemical Society* **2004,** *126* (13), 4366-4374.
41. Crudden, C. M.; Horton, J. H.; Ebralidze, I. I.; Zenkina, O. V.; McLean, A. B.; Drevniok, B.; She, Z.; Kraatz, H. B.; Mosey, N. J.; Seki, T.; Keske, E. C.; Leake, J. D.; Rousina-Webb, A.; Wu, G., Ultra stable self-assembled monolayers of N-heterocyclic carbenes on gold. *Nat Chem* **2014,** *6* (5), 409-414.
42. Hanrath, T.; Veldman, D.; Choi, J. J.; Christova, C. G.; Wienk, M. M.; Janssen, R. A. J., PbSe Nanocrystal Network Formation during Pyridine Ligand Displacement. *ACS applied materials & interfaces* **2009,** *1* (2), 244-250.
43. Leatherdale, C. A.; Kagan, C. R.; Morgan, N. Y.; Empedocles, S. A.; Kastner, M. A.; Bawendi, M. G., Photoconductivity in CdSe quantum dot solids. *Phys. Rev. B* **2000,** *62* (4), 2669-2680.
44. Sun, Y. G.; Rogers, J. A., Inorganic semiconductors for flexible electronics. *Adv. Mater.* **2007,** *19* (15), 1897-1916.
45. Tang, J. A.; Sargent, E. H., Infrared Colloidal Quantum Dots for Photovoltaics: Fundamentals and Recent Progress. *Adv. Mater.* **2011,** *23* (1), 12-29.
46. Tisdale, W. A.; Williams, K. J.; Timp, B. A.; Norris, D. J.; Aydil, E. S.; Zhu, X. Y., Hot-Electron Transfer from Semiconductor Nanocrystals. *Science* **2010,** *328* (5985), 1543-1547.
47. Yu, D.; Wang, C. J.; Wehrenberg, B. L.; Guyot-Sionnest, P., Variable range hopping conduction in semiconductor nanocrystal solids. *Physical Review Letters* **2004,** *92* (21), 216802.
48. Zillner, E.; Fengler, S.; Niyamakom, P.; Rauscher, F.; Kohler, K.; Dittrich, T., Role of Ligand Exchange at CdSe Quantum Dot Layers for Charge Separation. *Journal of Physical Chemistry C* **2012,** *116* (31), 16747-16754.
49. Ahrland, S.; Chatt, J.; Davies, N. R.; Williams, A. A., The Relative Affinities of an Amine, an Organic Phosphine, and a Sulphide for Cadmium Ion. *J Chem Soc* **1958,** (Apr), 1403-1405.
50. Ahrland, S.; Chatt, J.; Davies, N. R., The Relative Affinities of Ligand Atoms for Acceptor Molecules and Ions. *Q Rev Chem Soc* **1958,** *12* (3), 265-276.

51. Smith, A. M.; Johnston, K. A.; Crawford, S. E.; Marbella, L. E.; Millstone, J. E., Ligand density quantification on colloidal inorganic nanoparticles. *Analyst* **2017,** *142* (1), 11-29.
52. Beecher, A. N.; Yang, X.; Palmer, J. H.; LaGrassa, A. L.; Juhas, P.; Billinge, S. J. L.; Owen, J. S., Atomic Structures and Gram Scale Synthesis of Three Tetrahedral Quantum Dots. *Journal of the American Chemical Society* **2014,** *136* (30), 10645-10653.
53. Strong, L.; Whitesides, G. M., Structures of Self-Assembled Monolayer Films of Organosulfur Compounds Adsorbed on Gold Single-Crystals - Electron-Diffraction Studies. *Langmuir* **1988,** *4* (3), 546-558.
54. Offord, D. A.; Griffin, J. H., Kinetic Control in the Formation of Self-Assembled Mixed Monolayers on Planar Silica Substrates. *Langmuir* **1993,** *9* (11), 3015-3025.
55. Offord, D. A.; Leonard, W. G.; Griffin, J. H., Self-Assembled Mixed Monolayers of Long-Chain and Very Short-Chain Adsorbates on Silica and Gold Surfaces. *Abstr Pap Am Chem S* **1993,** *205*, 219-Orgn.
56. Ulman, A., Formation and structure of self-assembled monolayers. *Chem Rev* **1996,** *96* (4), 1533-1554.
57. Folkers, J. P.; Laibinis, P. E.; Whitesides, G. M., Self-Assembled Monolayers of Alkanethiols on Gold - Comparisons of Monolayers Containing Mixtures of Short-Chain and Long-Chain Constituents with Ch3 and Ch2oh Terminal Groups. *Langmuir* **1992,** *8* (5), 1330-1341.
58. Somasundaran, P.; Huang, L., Adsorption/aggregation of surfactants and their mixtures at solid-liquid interfaces. *Adv Colloid Interfac* **2000,** *88* (1-2), 179-208.
59. Wong, K. T.; Lewis, N. S., What a Difference a Bond Makes: The Structural, Chemical, and Physical Properties of Methyl-Terminated Si(111) Surfaces. *Accounts Chem Res* **2014,** *47* (10), 3037-3044.
60. Malyk, S.; Shalhout, F. Y.; O'Leary, L. E.; Lewis, N. S.; Benderskii, A. V., Vibrational Sum Frequency Spectroscopic Investigation of the Azimuthal Anisotropy and Rotational Dynamics of Methyl-Terminated Silicon(111) Surfaces. *Journal of Physical Chemistry C* **2013,** *117* (2), 935-944.
61. Yang, Y. A.; Wu, H.; Williams, K. R.; Cao, Y. C., Synthesis of CdSe and CdTe Nanocrystals without Precursor Injection. *Angewandte Chemie International Edition* **2005,** *44* (41), 6712-6715.
62. Marsi, K. L., Stereochemistry of some reactions of phospholane derivatives. *Journal of the American Chemical Society* **1969,** *91* (17), 4724-4729.

TOC Graphic